JACS
JOURNAL OF THE AMERICAN CHEMICAL SOCIETY
pubs.acs.org/JACS
Article

Rational Design of Bright Long Fluorescence Lifetime Dyad Fluorophores for Single Molecule Imaging and Detection

Laura Kacenauskaite, Niels Bisballe, Rebecca Mucci, Marco Santella, Tönu Pullerits, Junsheng Chen, Tom Vosch,* and Bo W. Laursen*

Cite This: J. Am. Chem. Soc. 2021, 143, 1377−1385
Read Online
ACCESS | Metrics & More | Article Recommendations | Supporting Information

ABSTRACT: Increasing demand for detecting single molecules in challenging environments has raised the bar for the fluorophores used. To achieve better resolution and/or contrast in fluorescence microscopy, it is now essential to use bright and stable dyes with tailored photophysical properties. While long fluorescence lifetime fluorophores offer many advantages in time-resolved imaging, their inherently lower molar absorption coefficient has limited applications in single molecule imaging. Here we propose a generic approach to prepare bright, long fluorescence lifetime dyad fluorophores comprising an absorbing antenna chromophore with high absorption coefficient linked to an acceptor emitter with a long fluorescence lifetime. We introduce a dyad consisting of a perylene antenna and a triangulenium emitter with 100% energy transfer from donor to acceptor. The dyad retained the long fluorescence lifetime (∼17 ns) and high quantum yield (75%) of the triangulenium emitter, while the perylene antenna increased the molar absorption coefficient (up to 5 times) in comparison to the free triangulenium dye. These triangulenium based dyads with significantly improved brightness can now be detected at the single molecule level and easily discriminated from bright autofluorescence by time-gated and other lifetime-based detection schemes.

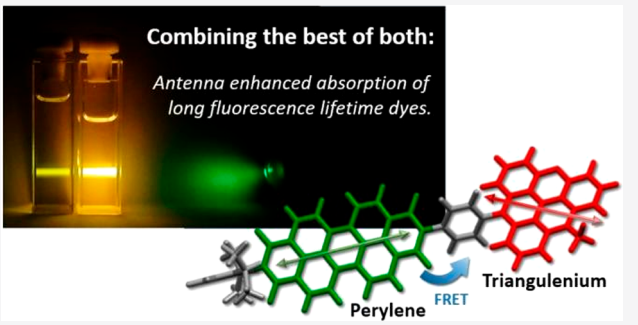

INTRODUCTION

In the past decades, significant improvements in fluorescence microscopy pushed the spatial resolution beyond the diffraction limit.[1] These advanced, fluorescence-based microscopy methods are now able to resolve single molecules and their interactions on a scale of a few nanometers.[2] Several of these techniques require special photophysical properties of the fluorophores.[3,4] As the role of tailored fluorophores becomes more important in various fields of imaging and sensing, there is an increasing interest in emitters with long fluorescence lifetimes which enable more efficient time-gated (TG) detection and provide a wider dynamic range for fluorescence anisotropy and FLIM-based applications.[5−8]

In order to optimize the performance of organic fluorophores, usually a few rational design approaches are used. While the spectral range of the fluorophore can be tuned by modifying the conjugated system, quantum yield (and subsequently, brightness) can be increased significantly by chemically introducing rigidity in the backbone or adding side groups to the fluorophore (reducing the nonradiative decay rate or preventing self-quenching).[9−16] Mainly based on these approaches, an extensive library of organic fluorophores was developed over the years. Some well-known commercial fluorophores including Alexa, Atto, cyanine, and rhodamine based dyes (Supporting Information, Table S1) are characterized in terms of fluorescence lifetime and absorption coefficient in Figure 1 and plotted as black dots. Most of the dyes are very bright and display a limited fluorescence lifetime in a similar range as the autofluorescence of biological samples (<5 ns).[17,18] To be able to fully exploit the attractive possibilities of time-resolved techniques, fluorophores with significantly longer fluorescence lifetimes are required.

One such class of dyes is trianguleniums, which are planar and rigid carbocations with tunable absorption and emission wavelengths, high fluorescence quantum yields, and lifetimes as long as 23 ns.[20−24] Even though most of the red long fluorescence lifetime emitters of this class have surprisingly high quantum yield values, the price for its extended fluorescence lifetime is a reduced absorption coefficient. It was previously reported that the molar absorption coefficient of the long fluorescence lifetime triangulenium dyes (like DAOTA, ADOTA, or CDATA, $\tau \approx 15-22$ ns) lies around $\varepsilon \approx 15\,000-20\,000$ $M^{-1}\cdot cm^{-1}$.[20,25] On the other hand, the

Received: September 30, 2020
Published: January 11, 2021

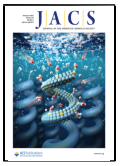

https://doi.org/10.1021/jacs.0c10457
J. Am. Chem. Soc. 2021, 143, 1377−1385

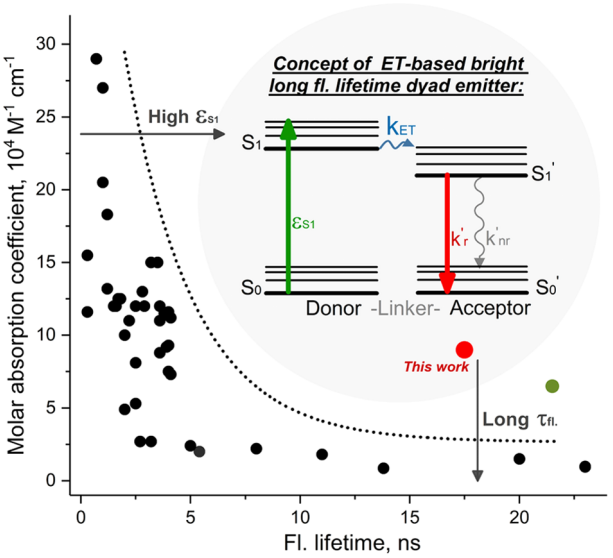

Figure 1. Practical representation of the concept of the "ideal" bright, long fluorescence lifetime dyad fluorophore (insert). Black dots in the graph represent various common, commercially available fluorophores and the relation between their molar absorption coefficient (at λ_{max}) and observed fluorescence lifetimes. Green dot: result from Osaki et al.[19] Red dot: PDI-DAOTA dyad reported here.

majority of the fluorophores that were designed to be bright (brightness = $\varepsilon_\lambda\Phi$) have short fluorescence lifetimes ($\tau < 5$ ns) and reach molar absorption coefficients of $\varepsilon \approx 100\,000$ $M^{-1}\cdot cm^{-1}$ or more; see Figure 1. These values of fluorescence lifetimes and absorption coefficients reflect that inherently the radiative lifetime (τ/Φ) and molar absorption coefficient (ε) are inversely proportional to each other according to the Strickler–Berg law.[26]

To overcome this limitation, it is necessary to find an approach to engineer the two parameters independently. From the perspective of the molecular design, an ideal way to bypass the Strickler–Berg law would be a three-level system, where absorption and emission happens to/from different electronic states. However, independent engineering of excited states (S_n and S_1) in the same conjugated framework is very difficult. As an alternative, a way to overcome these limitations was proposed by Osaki et al., reporting a strongly absorbing anthracene dimer which forms excimers acting as long fluorescence lifetime emitters.[19] These dimers were shown to provide a lifetime of ~22 ns together with molar absorption coefficient comparable to other widely used fluorophores ($\varepsilon \approx$ 40 000–60 000 M^{-1} cm^{-1}, Figure 1, green dot). Even longer fluorescence lifetimes (up to ~170 ns[27]) were observed by utilizing the same approach on anthracene crystals. However, despite significant improvement, this emitter concept suffers from multiexponential fluorescence decays, low water solubility, and difficulty of further engineering of, for example, wavelength and fluorescence lifetime, as it relies on an environment dependent dimerization in the excited state. Similar design complications would arise for ground state H-aggregates that also can lead to a system with high molar absorption coefficient and long fluorescence lifetimes.[28,29]

Here we propose another, more generic approach to obtain high brightness and long fluorescence lifetime emitters without relying on structural rearrangements. Covalent coupling of two fluorophores (one acting as highly absorbing antenna and another as long fluorescence lifetime emitter) yields an efficient Förster resonance energy transfer (FRET) pair. Even though the coupling of two or more fluorescent dyes in FRET dyads or triads is common in the literature as an approach to investigate energy transfer pathways,[30−34] increase the Stokes shift of the fluorescent probe[35,36] or brightness of phosphorescent lanthanide complexes,[37] to our knowledge this is the first time a dyad was specifically synthesized to combine a high absorbing antenna with a long fluorescence lifetime organic acceptor dye (Figure 1, insert). By choosing the right pair of organic dyes and appropriate linker, a system with efficient energy transfer, outcompeting the other deactivation pathways in the antenna, should be possible to achieve. This approach also has a large potential advantage of being very flexible in terms of the final dyad. In theory, a huge variety of different dyads with predictable absorbance/emission wavelengths and emission lifetimes can be assembled from known chromophores.

To test this dyad concept for making bright long fluorescence lifetime organic dyes, we selected a stable, long fluorescence lifetime triangulenium dye (diazaoxatriangulenium, DAOTA) that was coupled with perylene derivatives. This combination provides good spectral overlap, an acceptor with long fluorescence lifetime, and strongly absorbing perylenes that were already widely tested in FRET pairs.[38−41] A phenyl bridge was chosen as a linker between these two moieties as it is short, rigid, and nonquenching. The key challenge in the design is to obtain highly efficient energy transfer, yet securing weak electronic coupling between the donor and acceptor to avoid significant perturbation of the individual chromophores that could compromise the high quantum yield or long fluorescence lifetime of the emitter. For the two synthesized perylene-DAOTA dyads, PMI-DAOTA and PDI-DAOTA (Figure 2), we indeed found these desired properties and near perfect retention of the high quantum yield and long fluorescence lifetime of the DAOTA emitter. This

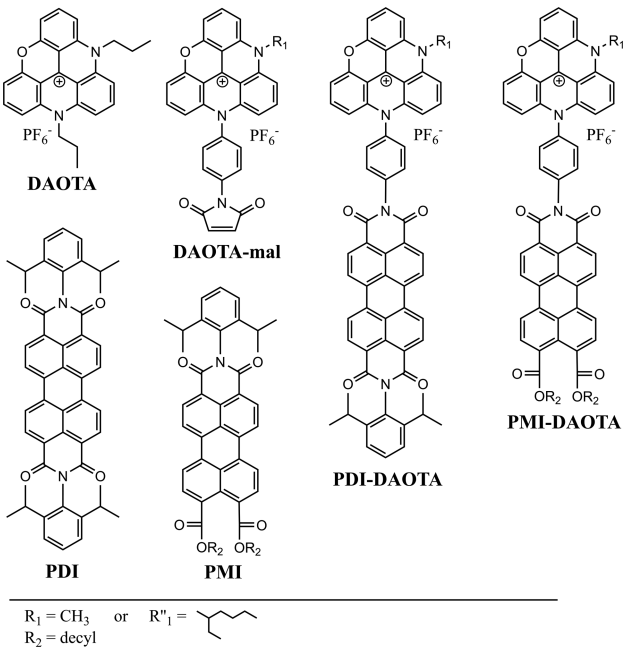

Figure 2. Structures of the synthesized dyads (PDI-DAOTA and PMI-DAOTA) and their individual building blocks (PDI, PMI, DAOTA, and DAOTA-mal) that act as reference compounds in the characterization of the dyads' photophysical properties.

https://doi.org/10.1021/jacs.0c10457
J. Am. Chem. Soc. 2021, 143, 1377−1385

leads to a ≈5-fold increase in the brightness compared to the native DAOTA dye, allowing us to demonstrate fluorescence-based time-gated single molecule imaging of the dyads.

RESULTS AND DISCUSSION

Molecular Design and Synthesis of the Dyads. As a model to present the concept of improved brightness and long fluorescence lifetime emission, perylene diimide (PDI) and perylene monoimide (PMI) were chosen as the absorbing antenna and hence energy donors in the two dyads: PDI-DAOTA and PMI-DAOTA. Figure 2 shows the structure of the dyads and the reference compounds used in the spectroscopic characterization of the dyads. For the acceptor, the simple propyl substituted DAOTA was used as a control.[42,43] Additionally, also DAOTA-mal[44] (maleimide functionalized DAOTA) was used as a reference compound to investigate the effect of the R_1 group and the linker on the overall photophysical properties.

The two dyads were synthesized by condensation of DAOTA-anilines with perylene monoanhydrides in imidazole at elevated temperatures. Detailed synthetic procedures and characterization are given in Supporting Information.

As indicated in Figure 2, two sets of dyads, containing different side groups (R_1 or R''_1) were synthesized and investigated. Methyl-substituted dyads, even though structurally very simple, rigid, and planar, have low solubility in most solvents. In order to improve the solubility of these molecules, the methyl group in the R_1 position was replaced by the branched, medium long ethyl-hexyl alkyl chain (R''_1). This modification improved solubility in a broad variety of water-miscible solvents like methanol, acetonitrile, tetrahydrofuran, etc. In the following section both PMI and PDI containing dyads with methyl-functionalized DAOTA will be discussed. The analysis of the ethyl-hexyl substituted (R''_1) PMI/PDI-DAOTA dyads can be found in the Supporting Information (Figure S1). In short, the data show that substitution in R_1 position in DAOTA unit does not change the photophysical properties of the dyad significantly and can be used to adjust the solubility or chemical properties.

Photophysical Properties of the Dyads. Figure 3 shows absorption and emission spectra of the dyads compared to their individual constituents, while key parameters are tabulated in Table 1. First, both free PDI (abs 525 nm, em 535 nm) and PMI (abs 505 nm, em 525 nm) show their characteristic sharp absorption and emission peaks previously reported and well-documented in the literature.[39] Also, DAOTA-mal shows the typical DAOTA[42] absorption and emission spectra (abs 560 nm, em 580 nm) as well as no significant changes of the fluorescence quantum yields and fluorescence lifetimes (Φ = 78%, τ = 20.2 ns), demonstrating that the introduction of phenyl-imide moiety does not affect DAOTA's photophysical properties.

In the absorption spectra of the dyads, the main features match the spectral shape of the individual components; however, the absorption peaks of both antennas are slightly red-shifted (~166 cm^{-1} for the PDI containing dyad and ~177 cm^{-1} for the PMI dyad) in comparison to the reference compounds PDI and PMI. Similar shifts in perylene-type molecules were also previously observed upon substitution with bulky side groups.[45,46] It is most likely the result of weak electronic coupling between the chromophores at such a short distance, as predicted by Förster.[47,48] The absorption peak in

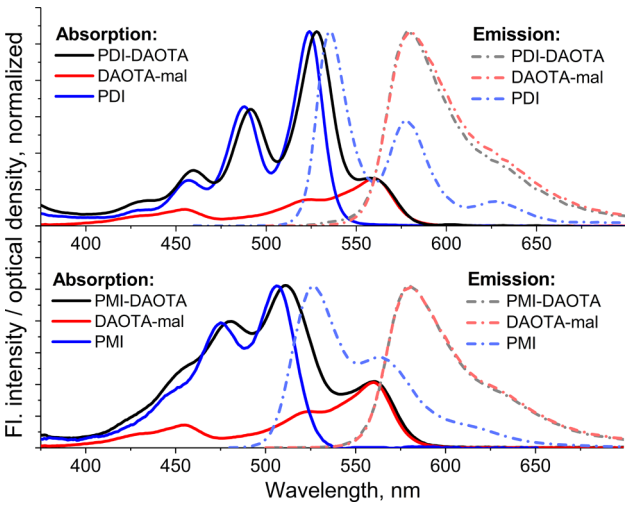

Figure 3. Absorption and emission spectra of the PDI-DAOTA and PMI-DAOTA dyads and the reference compounds PDI, PMI, and DAOTA-mal in DCM. Emission spectra were recorded while exciting at 470 nm.

the dyads that belongs to the DAOTA unit (~560 nm), on the other hand, is unchanged upon conjugation with the perylenes.

The emission spectra of the dyads, while exciting the antennas (525 and 505 nm in the cases of PDI and PMI, respectively), are practically identical to the fluorescence spectrum of DAOTA-mal (excited at 560 nm, Figure 3). No emission from the antenna is observed in the dyads, meaning that energy transfer efficiently outcompetes radiative decay in the antennas. Normalized excitation and emission spectra measured every 5 nm (Figure 4 and Figure S2) are practically invariant, confirming that dyads are pure. The close resemblance of the absorption spectra to the excitation spectra across the visible range (Figure 4) shows that the same quantum yield of fluorescence is obtained no matter if excitation takes place directly in the DAOTA emitter or via the perylene antenna, leading to the conclusion that the efficiency of energy transfer is close to 100%. Analogous results were observed for branched alkyl chain functionalized (R''_1) PMI/PDI-DAOTA dyads.

Fluorescence decay curves (Figure S3) obtained for both dyads by exciting the antenna fit very well with a single-exponential decay model, resolving lifetimes of 17.6 and 16.6 ns for the PMI and PDI containing dyad, respectively. These fluorescence lifetimes of the DAOTA unit in the dyads are only slightly lower than the lifetime of the DAOTA-mal (20.2 ns) reference compound. This decrease in fluorescence lifetime is accompanied by a small reduction of quantum yield, and we tentatively assign this to a slight increase of the nonradiative deactivation in the larger dyad molecules. Furthermore, it can be seen that no donor emission or energy transferring components can be detected, as the transfer rate is faster than the instrument response function (fwhm ≈ 200 ps).

Transient Absorption Studies and FRET Rate. To obtain a more detailed understanding of the energy transfer process between perylene antenna and the DAOTA emitter, transient absorption (TA) measurements were performed on PMI-DAOTA dyad in DCM with a 510 nm pump (excitation) and white light probe. TA spectra of individual components (PMI and DAOTA) can be found in Supporting Information, Figure S4. For the dyad the locally excited state on the PMI

https://doi.org/10.1021/jacs.0c10457
J. Am. Chem. Soc. 2021, 143, 1377−1385

Table 1. Summary of Photophysical Properties of the Dyads and the Reference Compounds

	DAOTA	DAOTA-mal	PMI/PDI	PMI/PDI-DAOTA	
solvent DCM	ex 510 nm, em 580 nm	ex 510 nm, em 580 nm	ex 510 nm, em 540 nm	ex 510 nm, em 580 nm	ex 560 nm, em 580 nm
molar absorption coef (ε), cm^{-1} M^{-1} at λ_{max}	18500	16400	60000/91000	56700/92000	24500/26000
Fl lifetime (τ), ns	21.2	20.2	4.1/3.6	17.5/16.6	17.4/17.2
quantum yield (Φ), %	80	78		73/75	
limiting anisotropy (r_0)	0.39	0.38	0.38/0.39	0.27/0.27	0.36/0.36
angle between abs and em transition dipole moments (β), deg	~0	~0	~0/~0	30/30	~0/~0

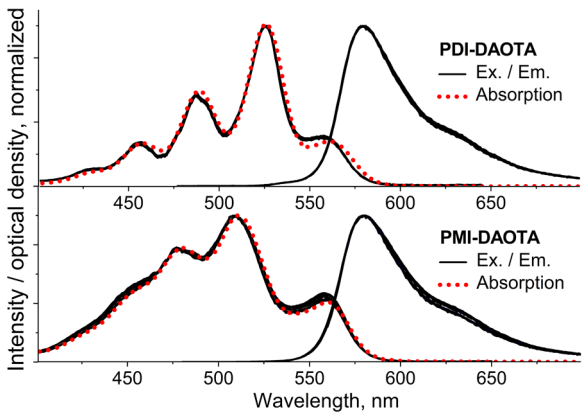

Figure 4. Normalized fluorescence excitation and emission spectra of the dyads, measured every 5 nm throughout corresponding range. Red dotted curve represents absorption spectrum of each dyad.

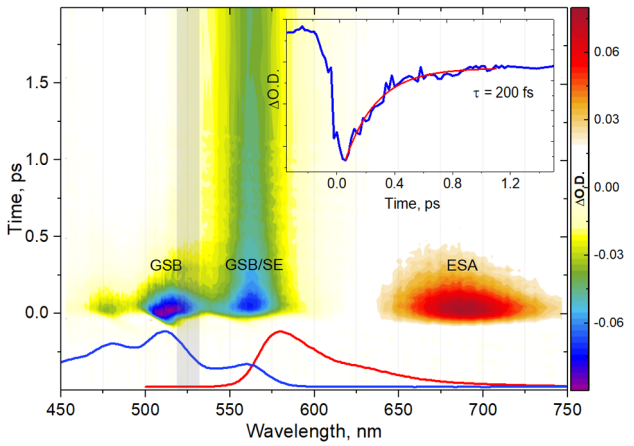

Figure 5. TA spectra (510 nm pump) of PMI-DAOTA dyad in DCM together with its steady state absorption (blue line) and emission (red line) spectra. Upper inset shows ground state bleaching (GSB) rate at 525 nm (integrated over gray band), fitted with monoexponential decay model (red curve).

antenna is clearly observed right after excitation (Figure 5) as a ground-state bleaching (GSB) of the PMI absorption peak (at 510 nm) and excited state absorption (ESA) at 700 nm (additional TA plots are given in Figure S5). Both these signals decay extremely fast with time constants of ~200 fs (Figure 5, insert) and ~210 fs (Figure S4), respectively. As the pump pulse has a width of ~100 fs, we can conclude that the local PMI excited state in the dyad has a very short lifetime of $\tau_{PMI*} \approx 200$ fs. The locally excited state on the DAOTA emitter is formed on a similar time scale (Figure S5C) and remains for nanoseconds (Figure S4F), in agreement with the fluorescence lifetime measurements (Table 1). The very short lifetime of the locally excited PMI state and 100% energy transfer allow us to calculate the rate of energy transfer to the DAOTA chromophore as $k_{ET} = 1/\tau_{PMI*} = 5 \times 10^{12}$ s^{-1}, since this process is the only one responsible for deactivating PMI* in the dyad, as indicated in the Jablonski diagram in Figure 1.

On the basis of the energy transfer time constant (200 fs) and intrinsic fluorescence lifetime of PMI in DCM (4.1 ns), an energy transfer efficiency >99.995% can be calculated. This is in agreement with the nonobservable emission from the PMI antenna.

Applying the standard Förster model and a center-to-center distance between donor and acceptor of 14 Å, we calculated the expected energy transfer rate to be $k'_{ET} = 1.2 \times 10^{12}$ s^{-1} (details given in Supporting Information). This value is around 4 times lower than the experimental value and indicates limitations of the Förster point dipole approximation at short donor−acceptor distances and potential Dexter-type contributions.[34,49−52]

In other perylene based dyads similar fast transfer rates were found with conservation of the spectral properties of the individual constituents, indicative of weak electronic coupling.[53] The PMI/PDI-DAOTA dyads reported here also preserve their local excited states and transition dipole moments (see below) of the individual constituents. In this regard the dyad behaves similarly to a single organic dye where S_2 to S_1 internal conversion (ic) happens on a similar fast time scale and also with 100% efficiency, according to Kasha−Vavilov's rule.[54]

Table 1 summarizes information about absorption and emission maxima, absorption coefficients, fluorescence lifetimes, quantum yields, limiting anisotropies, and angles between the transition dipole moments in the dyads and the reference compounds. The reference compounds DAOTA and DAOTA-mal display similar fluorescence lifetimes, molar absorption coefficients, and quantum yields. This proves that substitution with different groups through the nitrogen bridges does not significantly affect the photophysical properties and that this approach can be used to produce similar dyads from other compatible fluorophores. Due to the antenna in the dyads, a drastic improvement in terms of molar absorption coefficients can be observed. The absorptivity and brightness of the dyads are up to 5 times higher (when exciting the maximum absorption in the antennas) in comparison to the free DAOTA chromophores, excited in the maximum absorption peak at 560 nm. This significant improvement now gives the DAOTA chromophore the opportunity to be used in applications where they were too dim to be used before. With high absorption coefficient and long excited state lifetime the dyads could be candidate systems for displaying exciton blockade.[55−57] However, we did not observe any signs

https://doi.org/10.1021/jacs.0c10457
J. Am. Chem. Soc. 2021, 143, 1377−1385

of such phenomena in the bulk or single molecule measurements (see below), which could be due to efficient annihilation if both constituents are in the excited state simultaneously.[58]

Fluorescence Anisotropy Studies. Bright molecules with long fluorescence lifetime are in high demand for polarization studies, as they can provide a significantly longer time frame to investigate nanoscale molecular motions.[59] In addition to long lifetime and high brightness, relatively high limiting anisotropy values are necessary to observe anisotropy changes over time. The dyads reported here could be beneficial for polarization studies as they still maintain relatively high anisotropy due to their rigid linker and the low angle between transition dipole moments in the antenna and emitter.

According to previous research, it is well established that perylenes as well as DAOTA have parallel absorption and emission transition dipole moments for their lowest energy transition, meaning that the limiting anisotropy for both individual components is close to the theoretical value of r_0 = 0.4.[59−62] However, due to the way the two molecules are coupled in the dyads, a certain angle between the "absorption" (perylene) and "emission" (DAOTA) transition dipole moments is introduced. Since both of them are planar and rigid structures, it is easy to theoretically calculate that the angle between these transition dipole moments should be around 30° in the dyads (see Figure S6). To confirm these calculations experimentally, Figure 6 shows steady-state fluorescence

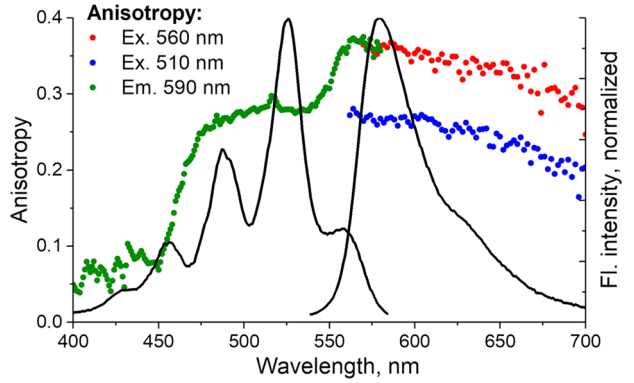

Figure 6. Fluorescence excitation and emission spectra (black lines, ex 525 nm, em 600 nm) and corresponding anisotropy spectra of the PDI-DAOTA dyad in a 95% glycerol/5% methanol mixture at −4 °C.

anisotropy spectra of one of the dyads PDI-DAOTA (R''_1) in a methanol/glycerol mixture. Fluorescence excitation and emission spectra plotted in the same graph confirm that an anisotropy value close to 0.4 can be obtained if the dyad is excited directly into the acceptor (DAOTA, 560 nm). However, after blue-shifting the excitation wavelength to where PDI absorption dominates, the emission anisotropy value drops to ∼0.27, in perfect agreement with an angle of 30° (see Supporting Information for details). These well-resolved anisotropy values confirm the structural rigidity of the dyad, as well as the integrity of the local transitions in the antenna and emitter units.

Single Molecule Studies of the Dyads. Even though in bulk the fluorescence intensity of the dyads was significantly increased in comparison to the simple DAOTA dyes, we wanted to see how these dyads act as single molecule emitters.[63−65] Figure 7 shows the dyads and the PMI/PDI reference compounds immobilized in a PMMA thin film. The

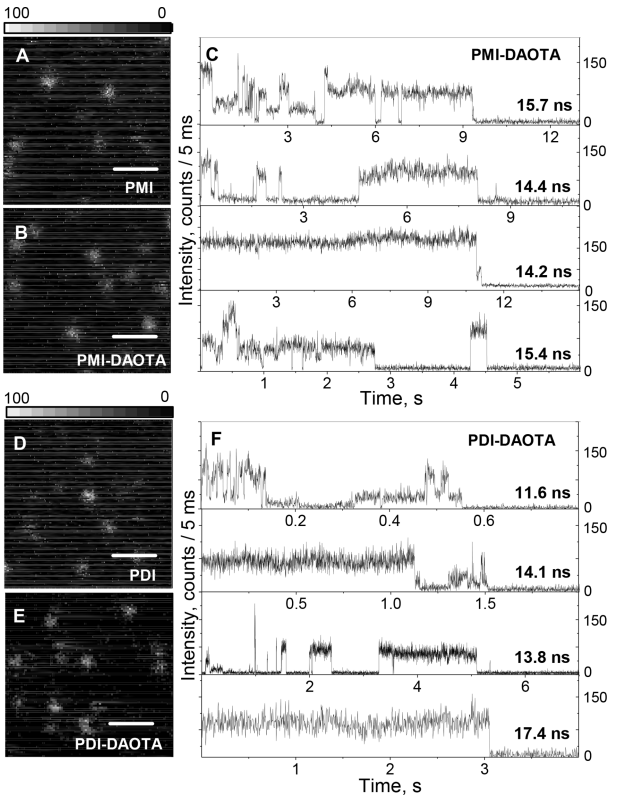

Figure 7. Single molecule studies of synthesized dyads (ex 510 nm, ∼300 W/cm^2, em >514 nm). (A/D) Single molecule fluorescence image of reference compounds PMI/PDI. (B/E) Single molecule fluorescence image of PMI/PDI-DAOTA dyads. Intensity scale, size, and scan rate are the same for all of the images. Scale bars indicate 1 μm. (C and F) Fluorescence intensity time traces and fluorescence lifetimes of a few dyad molecules from parts B and E, respectively.

scanning confocal fluorescence microscopy images in Figure 7 clearly show that intensitywise the dyads (B and E) are as bright as corresponding single PMI or PDI molecules (A and D). Attempts to obtain single molecule images of simple DAOTA dyes under similar conditions were unsuccessful due to too low brightness/signal.

The fluorescence intensity time traces (C and F) of selected dyads confirm that in addition to being bright they show the expected long fluorescence lifetimes of ∼12−17 ns of the DAOTA emitter (see Figure S7 for the corresponding decay curves).

On average, the single molecule fluorescence lifetimes of the dyads are slightly shorter than expected from the bulk measurements, but this could be due to the different polarity of PMMA versus DCM. Typical discrete on−off blinking and photobleaching of the dyads are observed as expected for single molecules. Surprisingly we do not observe a clear emission from the donor upon bleaching of the acceptor, as it is commonly observed in other dyads or triads.[30,66,67] The most likely explanation is that the bleached DAOTA acts as a quencher, since it is unlikely that the perylene dye (given its extremely short excited state lifetime of ∼200 fs) would bleach before the DAOTA. As a result, in this case, photostability of the dyad is limited by the stability of the acceptor. On the other hand, this ensures that the design goal of a long fluorescence lifetime emitter is maintained, even at the single molecule level and is not compromised by photobleaching. By use of DAOTA as an acceptor, the number of the emitted

https://doi.org/10.1021/jacs.0c10457
J. Am. Chem. Soc. 2021, 143, 1377−1385

photons is certainly high enough for single molecule imaging, even under demanding conditions (see below).

To show the advantages of using bright, long fluorescence lifetime emitters for imaging applications, time-gated confocal fluorescence microscopy and FLIM images of the dyads in samples with very high intensity background fluorescence were performed as a proof of concept experiment. A dilute PMI-DAOTA solution was mixed with a relatively high concentration of the PMI reference compound (approximately 30-fold excess) and immobilized in a PMMA film. Figure 8A shows

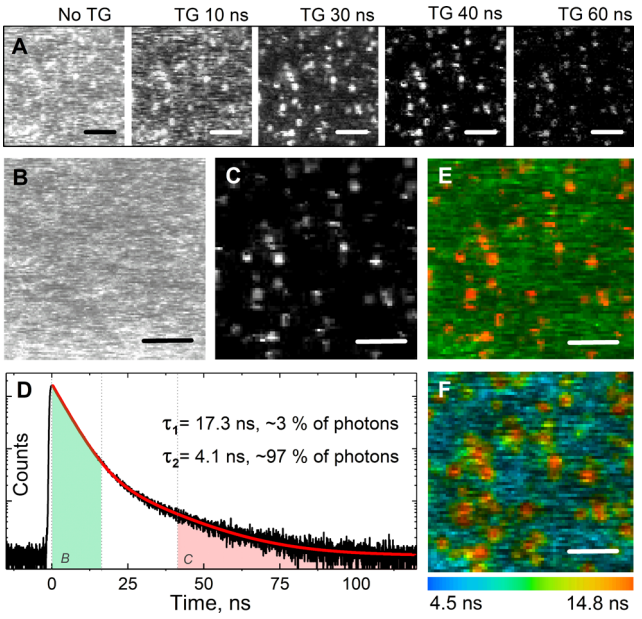

Figure 8. Time-resolved images (ex 510 nm, em >514 nm) of PMI-DAOTA dyad and PMI reference compound containing PMMA films. (A) Series of software-based, time-gated fluorescence intensity images. (B) Intensity image constructed out of photons that arrive during the first 17 ns after excitation (green time channel in graph D). (C) Time-gated fluorescence image corresponding to the red time channel in graph D. (D) Fluorescence decay curve constructed from all the photon arrival times in the image. (E) PArTI image (based on the green and red time channel in parts B and C). (F) FLIM image of the same area, where a monoexponential decay model was used to fit fluorescence decay curves for every pixel. Scale bars correspond to 1 μm.

time-gated fluorescence images of the PMI-DAOTA/PMI mixture with increasing time-gates (software based time-gating). The fluorescence decay curve obtained by summing up all photons from all the pixels (Figure 8D) clearly shows a multiexponential decay profile that can be fitted using a two-exponential decay model. Fluorescence lifetimes corresponding to the PMI reference compound (4.1 ns) and the PMI-DAOTA dyad (~17.3 ns) can be resolved, and the amplitudes of each component show that the PMI reference compound is responsible for as much as 97% of the total emission. For this reason, fluorescence imaging without time-gating (Figure 8A) looks rather homogeneous in intensity and no clear features can be resolved. However, when the time-gate (TG) is increased, spots corresponding to single dyad molecules start to become more and more visible, as the short fluorescence lifetime of the PMI does not contribute significantly anymore. When a time-gate corresponding to 40 ns is applied, almost no emission from the PMI can be detected and well resolved single dyad molecules can be seen.

Parts B, C, and E of Figure 8 show another method to visualize regions with different fluorescence lifetimes. Intensity images from the photons corresponding to the green time channel (Figure 8B) and the red time channel (Figure 8C) can be merged into a so-called PArTI (photon arrival time imaging) image (Figure 8E)[68] Here, the green color represents the photons that arrive during the first 17 ns after excitation, and orange areas (green + excess red in RGB format) correspond to the long fluorescence lifetime dyad emitters. Alternatively, the same data can also be represented as a FLIM image (Figure 8F), where an average single exponential decay value per pixel is represented by color. Depending on the application, the time-resolved fluorescence imaging techniques together with dyads with improved brightness can open up new possibilities for fluorescence-based single molecule imaging of samples where high autofluorescence levels are a limiting factor.

CONCLUSION

We report a generic approach to design bright organic dyes with long fluorescence lifetime. Long fluorescence lifetimes and high brightness are achieved by synthesizing a dyad containing a highly absorbing antenna and a long fluorescence lifetime acceptor/emitter. Here we show that perylene-triangulenium dyads synthesized via this approach yield 100% energy transfer. In addition, such fluorophores retain their single-exponential fluorescence decay, high quantum yield, and anisotropy values, making them attractive candidates for removing high background in time-gated confocal fluorescence imaging, FLIM, or anisotropy studies.

ASSOCIATED CONTENT

Supporting Information

The Supporting Information is available free of charge at https://pubs.acs.org/doi/10.1021/jacs.0c10457.

Experimental section; synthetic procedures and characterization of new compounds; characterization of photophysical properties of the ethyl-hexyl substituted (R''_1) PMI/PDI-DAOTA dyads; fluorescence lifetime decay histograms and decay fits, non-normalized emission spectra, theoretical calculation of limiting anisotropy values for perylene-triangulenium dyads; single dyad molecule fluorescence decay histograms and their fits (PDF)

AUTHOR INFORMATION

Corresponding Authors

Tom Vosch − *Nano-Science Center & Department of Chemistry, University of Copenhagen, 2100 Copenhagen, Denmark;* orcid.org/0000-0001-5435-2181; Email: tom@chem.ku.dk

Bo W. Laursen − *Nano-Science Center & Department of Chemistry, University of Copenhagen, 2100 Copenhagen, Denmark;* orcid.org/0000-0002-1120-3191; Email: bwl@chem.ku.dk

Authors

Laura Kacenauskaite − *Nano-Science Center & Department of Chemistry, University of Copenhagen, 2100 Copenhagen, Denmark*

Niels Bisballe − *Nano-Science Center & Department of Chemistry, University of Copenhagen, 2100 Copenhagen, Denmark;* orcid.org/0000-0002-4476-5481
Rebecca Mucci − *Nano-Science Center & Department of Chemistry, University of Copenhagen, 2100 Copenhagen, Denmark*
Marco Santella − *Nano-Science Center & Department of Chemistry, University of Copenhagen, 2100 Copenhagen, Denmark*
Tönu Pullerits − *Chemical Physics & NanoLund, Department of Chemistry, Lund University, 22100 Lund, Sweden;* orcid.org/0000-0003-1428-5564
Junsheng Chen − *Nano-Science Center & Department of Chemistry, University of Copenhagen, 2100 Copenhagen, Denmark; Chemical Physics & NanoLund, Department of Chemistry, Lund University, 22100 Lund, Sweden;* orcid.org/0000-0002-2934-8030

Complete contact information is available at: https://pubs.acs.org/10.1021/jacs.0c10457

Author Contributions

The manuscript was written through contributions of all authors. All authors have given approval to the final version of the manuscript.

Notes

The authors declare the following competing financial interest(s): Bo W. Laursen is associated with the company KU-dyes, which produces and sells fluorescent dyes (including triangulenium dyes).

■ ACKNOWLEDGMENTS

Authors are grateful to Danish Council of Independent Research for financial support (Grant DFF-6111-00483).

■ ABBREVIATIONS

FRET, Förster resonance energy transfer; DAOTA, diazaoxatriangulenium; ADOTA, azadioxatriangulenium; CDATA, carbon-bridged triangulenium; PDI, perylene diimide; PMI, perylene monoimide; vis−NIR, visible−near infrared; fwhm, full width at half-maximum; TA, transient absorption; FLIM, fluorescence lifetime imaging microscopy; TG, time gate; UV, ultraviolet; QY, quantum yield; DCM, dichloromethane; PMMA, poly(methyl methacrylate); PArTI, photon arrival time imaging

■ REFERENCES

(1) Hell, S. W. Far-field optical nanoscopy. *Science* **2007**, *316* (5828), 1153−1158.
(2) Moerner, W. E.; Orrit, M. Illuminating Single Molecules in Condensed Matter. *Science* **1999**, *283* (5408), 1670−1676.
(3) Betzig, E.; Patterson, G. H.; Sougrat, R.; Lindwasser, O. W.; Olenych, S.; Bonifacino, J. S.; Davidson, M. W.; Lippincott-Schwartz, J.; Hess, H. F. Imaging intracellular fluorescent proteins at nanometer resolution. *Science* **2006**, *313* (5793), 1642−1645.
(4) Hotta, J. I.; Fron, E.; Dedecker, P.; Janssen, K. P. F.; Li, C.; Mullen, K.; Harke, B.; Buckers, J.; Hell, S. W.; Hofkens, J. Spectroscopic Rationale for Efficient Stimulated-Emission Depletion Microscopy Fluorophores. *J. Am. Chem. Soc.* **2010**, *132* (14), 5021−5023.
(5) Berezin, M. Y.; Achilefu, S. Fluorescence Lifetime Measurements and Biological Imaging. *Chem. Rev.* **2010**, *110* (5), 2641−2684.
(6) Hall, M. D.; Yasgar, A.; Peryea, T.; Braisted, J. C.; Jadhav, A.; Simeonov, A.; Coussens, N. P. Fluorescence polarization assays in high-throughput screening and drug discovery: a review. *Methods Appl. Fluoresc.* **2016**, *4* (2), 022001.
(7) Zhang, K. Y.; Yu, Q.; Wei, H.; Liu, S.; Zhao, Q.; Huang, W. Long-Lived Emissive Probes for Time-Resolved Photoluminescence Bioimaging and Biosensing. *Chem. Rev.* **2018**, *118* (4), 1770−1839.
(8) Meyer-Almes, F. J. Fluorescence lifetime based bioassays. *Methods Appl. Fluoresc.* **2017**, *5* (4), 042002.
(9) Lei, Z.; Li, X.; Luo, X.; He, H.; Zheng, J.; Qian, X.; Yang, Y. Bright, Stable, and Biocompatible Organic Fluorophores Absorbing/Emitting in the Deep Near-Infrared Spectral Region. *Angew. Chem., Int. Ed.* **2017**, *56* (11), 2979−2983.
(10) Umezawa, K.; Matsui, A.; Nakamura, Y.; Citterio, D.; Suzuki, K. Bright, Color-Tunable Fluorescent Dyes in the Vis/NIR Region: Establishment of New "Tailor-Made" Multicolor Fluorophores Based on Borondipyrromethene. *Chem. - Eur. J.* **2009**, *15* (5), 1096−1106.
(11) Butkevich, A. N.; Mitronova, G. Y.; Sidenstein, S. C.; Klocke, J. L.; Kamin, D.; Meineke, D. N. H.; D'Este, E.; Kraemer, P.-T.; Danzl, J. G.; Belov, V. N.; Hell, S. W. Fluorescent Rhodamines and Fluorogenic Carbopyronines for Super-Resolution STED Microscopy in Living Cells. *Angew. Chem., Int. Ed.* **2016**, *55* (10), 3290−3294.
(12) Panchuk-Voloshina, N.; Haugland, R. P.; Bishop-Stewart, J.; Bhalgat, M. K.; Millard, P. J.; Mao, F.; Leung, W. Y.; Haugland, R. P. Alexa dyes, a series of new fluorescent dyes that yield exceptionally bright, photostable conjugates. *J. Histochem. Cytochem.* **1999**, *47* (9), 1179−1188.
(13) Song, X. Z.; Johnson, A.; Foley, J. 7-Azabicyclo[2.2.1]heptane as a Unique and Effective Dialkylamino Auxochrome Moiety: Demonstration in a Fluorescent Rhodamine Dye. *J. Am. Chem. Soc.* **2008**, *130* (52), 17652−17653.
(14) Lavis, L. D.; Raines, R. T. Bright ideas for chemical biology. *ACS Chem. Biol.* **2008**, *3* (3), 142−155.
(15) Grimm, J. B.; English, B. P.; Chen, J.; Slaughter, J. P.; Zhang, Z.; Revyakin, A.; Patel, R.; Macklin, J. J.; Normanno, D.; Singer, R. H.; Lionnet, T.; Lavis, L. D. A general method to improve fluorophores for live-cell and single-molecule microscopy. *Nat. Methods* **2015**, *12* (3), 244−250.
(16) Panchuk-Voloshina, N.; Haugland, R. P.; Bishop-Stewart, J.; Bhalgat, M. K.; Millard, P. J.; Mao, F.; Leung, W.-Y.; Haugland, R. P. Alexa Dyes, a Series of New Fluorescent Dyes that Yield Exceptionally Bright, Photostable Conjugates. *J. Histochem. Cytochem.* **1999**, *47* (9), 1179−1188.
(17) Zhang, K. Y.; Yu, Q.; Wei, H.; Liu, S.; Zhao, Q.; Huang, W. Long-Lived Emissive Probes for Time-Resolved Photoluminescence Bioimaging and Biosensing. *Chem. Rev.* **2018**, *118*, 1770−1839.
(18) Meyer-Almes, F.-J. Fluorescence lifetime based bioassays. *Methods Appl. Fluoresc.* **2017**, *5*, 042002.
(19) Osaki, H.; Chou, C. M.; Taki, M.; Welke, K.; Yokogawa, D.; Irle, S.; Sato, Y.; Higashiyama, T.; Saito, S.; Fukazawa, A.; Yamaguchi, S. A Macrocyclic Fluorophore Dimer with Flexible Linkers: Bright Excimer Emission with a Long Fluorescence Lifetime. *Angew. Chem., Int. Ed.* **2016**, *55* (25), 7131−7135.
(20) Rosenberg, M.; Rostgaard, K. R.; Liao, Z.; Madsen, A. O.; Martinez, K. L.; Vosch, T.; Laursen, B. W. Design, synthesis, and time-gated cell imaging of carbon-bridged triangulenium dyes with long fluorescence lifetime and red emission. *Chem. Sci.* **2018**, *9* (12), 3122−3130.
(21) Sørensen, T. J.; Laursen, B. W.; Luchowski, R.; Shtoyko, T.; Akopova, I.; Gryczynski, Z.; Gryczynski, I. Enhanced fluorescence emission of Me-ADOTA(+) by self-assembled silver nanoparticles on a gold film. *Chem. Phys. Lett.* **2009**, *476* (1−3), 46−50.
(22) Laursen, B. W.; Krebs, F. C. Synthesis, structure, and properties of azatriangulenium salts. *Chem.—Eur. J.* **2001**, *7* (8), 1773−1783.
(23) Laursen, B. W.; Krebs, F. C. Synthesis of a triazatriangulenium salt. *Angew. Chem., Int. Ed.* **2000**, *39* (19), 3432−3434.
(24) Bosson, J.; Gouin, J.; Lacour, J. Cationic triangulenes and helicenes: synthesis, chemical stability, optical properties and extended applications of these unusual dyes. *Chem. Soc. Rev.* **2014**, *43* (8), 2824−40.

(25) Thyrhaug, E.; Sørensen, T. J.; Gryczynski, I.; Gryczynski, Z.; Laursen, B. W. Polarization and Symmetry of Electronic Transitions in Long Fluorescence Lifetime Triangulenium Dyes. *J. Phys. Chem. A* **2013**, *117* (10), 2160−2168.
(26) Strickler, S. J.; Berg, R. A. Relationship between Absorption Intensity and Fluorescence Lifetime of Molecules. *J. Chem. Phys.* **1962**, *37* (4), 814−822.
(27) Hofmann, J.; Seefeld, K. P.; Hofberger, W.; Bässler, H. Excimers in solid non-crystalline anthracene. *Mol. Phys.* **1979**, *37* (3), 973−979.
(28) Laursen, B. W.; Reynisson, J.; Mikkelsen, K. V.; Bechgaard, K.; Harrit, N. 2,6,10-tris(dialkylamino)trioxatriangulenium salts: a new promising fluorophore. Ion-pair formation and aggregation in non-polar solvents. *Photochem. Photobio. Sci.* **2005**, *4* (8), 568−576.
(29) Liu, H.; Yao, L.; Li, B.; Chen, X.; Gao, Y.; Zhang, S.; Li, W.; Lu, P.; Yang, B.; Ma, Y. Excimer-induced high-efficiency fluorescence due to pairwise anthracene stacking in a crystal with long lifetime. *Chem. Commun.* **2016**, *52* (46), 7356−7359.
(30) Cotlet, M.; Vosch, T.; Habuchi, S.; Weil, T.; Müllen, K.; Hofkens, J.; De Schryver, F. Probing intramolecular Förster resonance energy transfer in a naphthaleneimide-peryleneimide-terrylenediimide-based dendrimer by ensemble and single-molecule fluorescence spectroscopy. *J. Am. Chem. Soc.* **2005**, *127* (27), 9760−9768.
(31) Heilemann, M.; Tinnefeld, P.; Mosteiro, G. S.; Parajo, M. G.; Van Hulst, N. F.; Sauer, M. Multistep energy transfer in single molecular photonic wires. *J. Am. Chem. Soc.* **2004**, *126* (21), 6514−6515.
(32) Bhalla, V.; Vij, V.; Tejpal, R.; Singh, G.; Kumar, M. Solvent dependent competition between fluorescence resonance energy transfer and through bond energy transfer in rhodamine appended hexaphenylbenzene derivatives for sensing of Hg2+ ions. *Dalton Transactions* **2013**, *42* (13), 4456−4463.
(33) Hinze, G.; Métivier, R.; Nolde, F.; Müllen, K.; Basché, T. Intramolecular electronic excitation energy transfer in donor/acceptor dyads studied by time and frequency resolved single molecule spectroscopy. *J. Chem. Phys.* **2008**, *128* (12), 124516.
(34) Curutchet, C.; Feist, F. A.; Averbeke, B. V.; Mennucci, B.; Jacob, J.; Müllen, K.; Basché, T.; Beljonne, D. Superexchange-mediated electronic energy transfer in a model dyad. *Phys. Chem. Chem. Phys.* **2010**, *12* (27), 7378−7385.
(35) Han, J.; Engler, A.; Qi, J.; Tung, C.-H. Ultra pseudo-Stokes shift near infrared dyes based on energy transfer. *Tetrahedron Lett.* **2013**, *54* (6), 502−505.
(36) Ren, T.-B.; Xu, W.; Zhang, W.; Zhang, X.-X.; Wang, Z.-Y.; Xiang, Z.; Yuan, L.; Zhang, X.-B. A General Method To Increase Stokes Shift by Introducing Alternating Vibronic Structures. *J. Am. Chem. Soc.* **2018**, *140* (24), 7716−7722.
(37) Junker, A. K. R.; Hill, L. R.; Thompson, A. L.; Faulkner, S.; Sørensen, T. J. Shining light on the antenna chromophore in lanthanide based dyes. *Dalton Transactions* **2018**, *47* (14), 4794−4803.
(38) Prathapan, S.; Yang, S. I.; Seth, J.; Miller, M. A.; Bocian, D. F.; Holten, D.; Lindsey, J. S. Synthesis and Excited-State Photodynamics of Perylene−Porphyrin Dyads. 1. Parallel Energy and Charge Transfer via a Diphenylethyne Linker. *J. Phys. Chem. B* **2001**, *105* (34), 8237−8248.
(39) Weil, T.; Vosch, T.; Hofkens, J.; Peneva, K.; Müllen, K. The Rylene Colorant Family-Tailored Nanoemitters for Photonics Research and Applications. *Angew. Chem., Int. Ed.* **2010**, *49* (48), 9068−9093.
(40) Kim, H. N.; Puhl, L.; Nolde, F.; Li, C.; Chen, L.; Basche, T.; Mullen, K. Energy Transfer at the Single-Molecule Level: Synthesis of a Donor−Acceptor Dyad from Perylene and Terrylene Diimides. *Chem.—Eur. J.* **2013**, *19* (28), 9160−9166.
(41) Langhals, H.; Esterbauer, A. J.; Walter, A.; Riedle, E.; Pugliesi, I. Förster Resonant Energy Transfer in Orthogonally Arranged Chromophores. *J. Am. Chem. Soc.* **2010**, *132*, 16777−16782.
(42) Bogh, S. A.; Simmermacher, M.; Westberg, M.; Bregnhøj, M.; Rosenberg, M.; De Vico, L.; Veiga, M.; Laursen, B. W.; Ogilby, P. R.; Sauer, S. P. A.; Sørensen, T. J. Azadioxatriangulenium and Diazaoxatriangulenium: Quantum Yields and Fundamental Photophysical Properties. *ACS Omega* **2017**, *2* (1), 193−203.
(43) Thyrhaug, E.; Sorensen, T. J.; Gryczynski, I.; Gryczynski, Z.; Laursen, B. W. Polarization and symmetry of electronic transitions in long fluorescence lifetime triangulenium dyes. *J. Phys. Chem. A* **2013**, *117* (10), 2160−2168.
(44) Bora, I.; Bogh, S. A.; Rosenberg, M.; Santella, M.; Sorensen, T. J.; Laursen, B. W. Diazaoxatriangulenium: synthesis of reactive derivatives and conjugation to bovine serum albumin. *Org. Biomol. Chem.* **2016**, *14* (3), 1091−1101.
(45) Shao, Y.; Zhang, X.; Liang, K.; Wang, J.; Lin, Y.; Yang, S.; Zhang, W.-B.; Zhu, M.; Sun, B. How does the interplay between bromine substitution at bay area and bulky substituents at imide position influence the photophysical properties of perylene diimides? *RSC Adv.* **2017**, *7* (26), 16155−16162.
(46) Mathew, S.; Johnston, M. R. The synthesis and characterisation of a free-base porphyrin-perylene dyad that exhibits electronic coupling in both the ground and excited states. *Chem. - Eur. J.* **2009**, *15* (1), 248−53.
(47) Valeur, B.; Berberan-Santos, M. N. Excitation Energy Transfer. In *Molecular Fluorescence*; Wiley-VCH, 2012; pp 213−261.
(48) Förster, T. *Delocalized Excitation and Excitation Transfer*; Florida State University, 1965.
(49) Muñoz-Losa, A.; Curutchet, C.; Krueger, B. P.; Hartsell, L. R.; Mennucci, B. Fretting about FRET: failure of the ideal dipole approximation. *Biophys. J.* **2009**, *96* (12), 4779−4788.
(50) Jiao, G.-S.; Thoresen, L. H.; Burgess, K. Fluorescent, Through-Bond Energy Transfer Cassettes for Labeling Multiple Biological Molecules in One Experiment. *J. Am. Chem. Soc.* **2003**, *125* (48), 14668−14669.
(51) Nelson, T.; Fernandez-Alberti, S.; Roitberg, A. E.; Tretiak, S. Conformational disorder in energy transfer: beyond Förster theory. *Phys. Chem. Chem. Phys.* **2013**, *15* (23), 9245−9256.
(52) Beljonne, D.; Curutchet, C.; Scholes, G. D.; Silbey, R. J. Beyond Förster Resonance Energy Transfer in Biological and Nanoscale Systems. *J. Phys. Chem. B* **2009**, *113* (19), 6583−6599.
(53) Métivier, R.; Nolde, F.; Müllen, K.; Basché, T. Electronic Excitation Energy Transfer between Two Single Molecules Embedded in a Polymer Host. *Phys. Rev. Lett.* **2007**, *98* (4), 047802.
(54) Kasha, M. Characterization of electronic transitions in complex molecules. *Discuss. Faraday Soc.* **1950**, *9* (0), 14−19.
(55) Vogelsang, J.; Cordes, T.; Forthmann, C.; Steinhauer, C.; Tinnefeld, P. Intrinsically Resolution Enhancing Probes for Confocal Microscopy. *Nano Lett.* **2010**, *10* (2), 672−679.
(56) Schönle, A.; Hänninen, P. E.; Hell, S. W. Nonlinear fluorescence through intermolecular energy transfer and resolution increase in fluorescence microscopy. *Ann. Phys.* **1999**, *8* (2), 115−133.
(57) Melnikov, S. M.; Yeow, E. K. L.; Uji-i, H.; Cotlet, M.; Müllen, K.; De Schryver, F. C.; Enderlein, J.; Hofkens, J. Origin of Simultaneous Donor−Acceptor Emission in Single Molecules of Peryleneimide−Terrylenediimide Labeled Polyphenylene Dendrimers. *J. Phys. Chem. B* **2007**, *111* (4), 708−719.
(58) Tinnefeld, P.; Hofkens, J.; Herten, D.-P.; Masuo, S.; Vosch, T.; Cotlet, M.; Habuchi, S.; Müllen, K.; De Schryver, F. C.; Sauer, M. Higher-Excited-State Photophysical Pathways in Multichromophoric Systems Revealed by Single-Molecule Fluorescence Spectroscopy. *ChemPhysChem* **2004**, *5* (11), 1786−1790.
(59) Sørensen, T. J.; Thyrhaug, E.; Szabelski, M.; Luchowski, R.; Gryczynski, I.; Gryczynski, Z.; Laursen, B. W. Azadioxatriangulenium (ADOTA(+)): A long fluorescence lifetime fluorophore for large biomolecule binding assay. *Methods Appl. Fluoresc.* **2013**, *1* (2), 025001.
(60) Maliwal, B. P.; Fudala, R.; Raut, S.; Kokate, R.; Sørensen, T. J.; Laursen, B. W.; Gryczynski, Z.; Gryczynski, I. Long-Lived Bright Red Emitting Azaoxa-Triangulenium Fluorophores. *PLoS One* **2013**, *8* (5), e63043.

(61) Johansson, L. B. A. Limiting fluorescence anisotropies of perylene and xanthene derivatives. *J. Chem. Soc., Faraday Trans.* **1990**, *86* (12), 2103−2107.
(62) Lakowicz, J. R. *Principles of Fluorescence Spectroscopy*; Springer US, 2006.
(63) Kudryavtsev, V.; Felekyan, S.; Woźniak, A. K.; König, M.; Sandhagen, C.; Kühnemuth, R.; Seidel, C. A. M.; Oesterhelt, F. Monitoring dynamic systems with multiparameter fluorescence imaging. *Anal. Bioanal. Chem.* **2006**, *387* (1), 71−82.
(64) Schlichting, P.; Duchscherer, B.; Seisenberger, G.; Basché, T.; Bräuchle, C.; Müllen, K. A Bichromophore Based on Perylene and Terrylene for Energy Transfer Studies at the Single-Molecule Level. *Chem. - Eur. J.* **1999**, *5* (8), 2388−2395.
(65) Dahan, M.; Laurence, T.; Pinaud, F.; Chemla, D. S.; Alivisatos, A. P.; Sauer, M.; Weiss, S. Time-gated biological imaging by use of colloidal quantum dots. *Opt. Lett.* **2001**, *26* (11), 825−827.
(66) Fron, E.; Puhl, L.; Oesterling, I.; Li, C.; Müllen, K.; De Schryver, F. C.; Hofkens, J.; Vosch, T. Energy Transfer Pathways in a Rylene-Based Triad. *ChemPhysChem* **2011**, *12* (3), 595−608.
(67) Haase, M.; Hübner, C. G.; Nolde, F.; Müllen, K.; Basché, T. Photoblinking and photobleaching of rylene diimide dyes. *Phys. Chem. Chem. Phys.* **2011**, *13* (5), 1776−1785.
(68) Liao, Z.; Tropiano, M.; Faulkner, S.; Vosch, T.; Sorensen, T. J. Time-resolved confocal microscopy using lanthanide centred near-IR emission. *RSC Adv.* **2015**, *5* (86), 70282−70286.

NOTE ADDED AFTER ISSUE PUBLICATION

This paper was published on January 11, 2021. Due to a technical reproduction error, Figure 7 did not display correctly. This has been corrected and the revised version was re-posted on May 3, 2021.

https://doi.org/10.1021/jacs.0c10457
J. Am. Chem. Soc. 2021, 143, 1377−1385